Scientific Reports

https://doi.org/10.1038/s41598-026-46634-3

Article in Press

Absence of synergistic effects by CDK12/13 inhibition in combination with cisplatin or olaparib in ovarian cancer cells

Received: 22 October 2025

Accepted: 26 March 2026

Published online: 01 April 2026

Cite this article as: Santer F.R., Hovdar L., Handle F. *et al.* Absence of synergistic effects by CDK12/13 inhibition in combination with cisplatin or olaparib in ovarian cancer cells. *Sci Rep* (2026). https://doi.org/10.1038/s41598-026-46634-3

Frédéric R. Santer, Lea Hovdar, Florian Handle, Irina Tsibulak, Verena Wieser, Michael J. Ausserlechner, Walther Parson, Simon Schnaiter, Alain G. Zeimet, Christian Marth & Heidelinde Fiegl

Absence of synergistic effects by CDK12/13 inhibition in combination with cisplatin or olaparib in ovarian cancer cells

Frédéric R. Santer[1,2*], Lea Hovdar[1*], Florian Handle[3*], Irina Tsibulak[1], Verena Wieser[1], Michael J. Ausserlechner[4], Walther Parson[5,6], Simon Schnaiter[7], Alain G. Zeimet[1*], Christian Marth[1*], Heidelinde Fiegl[1*]

[1]Department of Obstetrics and Gynecology, Medical University of Innsbruck, Innsbruck, Austria

[2]Department of Urology, Division of Experimental Urology, Medical University of Innsbruck, Innsbruck, Austria.

[3]Department of Pathology, Neuropathology and Molecular Pathology, Medical University of Innsbruck, Innsbruck, Austria.

[4]Department of Pediatrics I, Medical University Innsbruck, Innsbruck, Austria

[5]Institute of Legal Medicine, Medical University of Innsbruck, Innsbruck, Austria

[6]Forensic Science Program, The Pennsylvania State University, University Park, PA, USA

[7]Institute of Human Genetics, Medical University of Innsbruck, Innsbruck, Austria

* The authors contribute equally

Corresponding authors:

Christian Marth, Tel: +43 51250423051; Fax: +43 51250423055;

Email: Christian.Marth@i-med.ac.at

Alain Gustave Zeimet, Tel: +43 51250423051; Fax: +43 51250423055;

Email: Alain.Zeimet@i-med.ac.at

Heidelinde Fiegl, Tel: +43 51250423113; Fax: +43 51250423112;

Email: Heidelinde.Fiegl@i-med.ac.at

Department of Obstetrics and Gynecology, Medical University of Innsbruck, Innsbruck, Austria

Anichstr. 35, 6020 Innsbruck

Keywords: CDK12/13 inhibitor; SR-4835; ovarian cancer; platinum resistance; PARP inhibitor; synergism

Abbreviations:

CDK, Cyclin-dependent kinase; DDR, DNA damage response; HRD, homologous recombination repair deficiency; MTT 3-(4,5-Dimethyl-2-thiazolyl)-2,5-diphenyl-2H-tetrazolium bromide; OC, ovarian cancer; PARP, Poly (ADP-ribose) polymerase; PARPi, PARP inhibitors; poly(A), polyadenylation; qPCR, quantitative real-time PCR

Abstract

The identification of novel molecular drivers and the development of new state-of-the-art therapies are critical challenges in ovarian cancer (OC) treatment. Cyclin-dependent kinase 12 (CDK12) is a promising target, as it´s functional activity promotes genomic stability. Here, we examined the anticancer efficacy of the dual CDK12/13-inhibitor SR-4835 in platinum-sensitive and -resistant OC cell lines, as well as its potential as a drug partner for platinum or olaparib combination therapy. SR-4835 exhibited potent anti-proliferative effects on most OC cell lines with IC50 values within the nanomolar range. A tendency for increased sensitivity of the cisplatin-resistant compared to their sensitive, parental cell lines was observed. Transcriptome analyses indicated gross changes in gene expression in numerous signaling pathways by SR-4835. Gene downregulation was in part due to alternative exon usage, which correlated with the number of intronic polyadenylation sites per gene and gene length. Furthermore, SR-4835 lead to the downregulation of key homologous recombination pathway genes rendering a *BRCAness* phenotype. However, the combination of SR-4835 with cisplatin or olaparib primarily exhibited an additive, not synergistic, effect. In summary, the present findings indicate that CDK12/13 inhibitor SR-4835 has potent anti-cancer effects accompanied by a *BRCAness* induction, but fails to achieve synergistic effects with cisplatin or olaparib in OC cells.

INTRODUCTION

Epithelial ovarian cancer (OC) is the most lethal gynecological malignancy [1]. Although therapeutic options are becoming more personalized with increasing knowledge of histological and molecular features, intravenous doublet chemotherapy (platinum and taxane) remains the standard first-line therapy for advanced-stage OC [2,3]. In addition, poly (ADP-ribose) polymerase (PARP) inhibitors (PARPi) are approved by the European Medicines Agency (EMA) for maintenance treatment of advanced, platinum-responsive OC with high response rates in particular in *BRCA1/2*-mutated or homologous recombination deficiency (HRD)-positive patients [4,5]. However, innate or acquired resistance to platinum-based chemotherapy, and to PARPi, hampers the long-term survival of affected patients [6,7]. Strategies to overcome this constraint in the treatment of OC encompass the use of targeted therapies, non-platinum chemotherapies, and immunotherapies among others, either as single agent or in combination with approved therapies. Ideally, combination therapies should act synergistically at lower dosages than single agents thus lowering side effects and reducing the development of drug resistance. Since platinum-based therapies induce DNA damage, while PARPi interfere with the cell´s ability to repair DNA damage, a common combination approach for both platinum and PARPi therapies seeks a partner drug that is able to induce additional genomic instability.

One such candidate drug target is the cyclin-dependent kinase 12 (CDK12), which has functions in the regulation of transcription by phosphorylating the C-terminal domain (CTD) of RNA Polymerase II (RNAPII) and in maintaining genome stability [8]. Indeed, CDK12 loss-of-function mutations, occurring at a frequency of 1.9 – 4% in OC, are associated with the focal tandem-duplicator phenotype [9,10] and were shown to act as a synthetic lethality partner with PARP inhibitors in cell culture models [11]. CDK12, acting in a complex with cyclin K (CCNK), is crucial for the transcription of several DNA damage response (DDR) genes [12,13] thus disrupting HR-repair and resulting in a *BRCAness* phenotype [11,14,15]. This is linked to CDK12´s role in the non-recognition of intronic polyadenylation sites (IPA) important for the transcription of full-length transcripts [16,17]. Several studies reported promising results for CDK12/13 inhibitors across multiple tumor types [18–21]. ZSQ836, a dual CDK12/13 inhibitor was shown to have potent anticancer activity in OC cell culture and mouse models and to induce transcriptional

reprogramming, including downregulation of DDR genes [22]. Furthermore, this study demonstrated that CDK12 and CDK13 are ubiquitously expressed in human OC tissues, which is a critical requirement for the therapeutic application of CDK12/13 inhibition. Another dual CDK12/13 inhibitor, SR-4835, which acts as a molecular glue resulting in the degradation of CCNK and reduction of RNAPII phosphorylation has promising pre-clinical results in triple negative breast cancer (TNBC), melanoma and thyroid cancer cell line models [18,23,24]. Finally, the CDK12/13 inhibitor CT7439 has entered clinical Phase I/II trial in patients with solid malignancies (Clinicaltrials.gov ID: NCT06600789).

Here, we report on a comprehensive pre-clinical study testing the highly CDK12/13-specific inhibitor SR-4835 [18] in a panel of histologically differing OC cell lines models including cisplatin-resistant derivatives. We found that SR-4835 has potent anticancer activity in the nanomolar range in most cell lines tested including those with acquired cisplatin resistance. However, when used in a combination approach of SR-4835 with cisplatin or the PARPi olaparib, the growth inhibitory effects were largely additive only.

RESULTS

Effects of CDK12/13 inhibition on proliferation and gene expression

To investigate the effects of CDK12/13 inhibition by SR-4835 in OC cells, we selected as models of the disease cell lines with various histotypes of OC: the endometrioid A2780, the serous SK-OV-3 and the high-grade serous (HGSOC) Caov-3 cell lines. Additionally, we included two cisplatin-resistant derivatives, A2780 cis and Caov-3 cis. Of note, in a targeted exome sequencing approach no mutations in the target *CDK12* were found in either cell line (Supplementary Table 1). Using cell confluence measurements, we evaluated the sensitivity (IC50 concentrations) of the selected OC cell lines for inhibition of CDK12/13 by the small molecule SR-4835 (Fig. 1A). All cell lines had IC50 values below 100 nM SR-4835, with the exception of SK-OV-3 (IC50 = 279.3 nM). Interestingly, the cisplatin-resistant cell line A2780 cis (IC50: 37.73 nM) responded significantly better ($p<0.01$) to SR-4835 than the cisplatin-sensitive

A2780 (IC50: 64.77 nM) (Supplementary Fig. 1). A much smaller and non-significant effect was observed for the Caov-3/Caov-3 cis pair (IC50: 45.57 vs 40.07, respectively, p=0.4502).

Next, we studied how CDK12/13 inhibition by SR-4835 affects gene expression in OC cell lines. To mimic a near-patient treatment dosage and duration situation, we chose for transcriptome analysis 90 nM SR-4835 (corresponding to approx. double median IC50 concentration of the previously tested cell lines) and 24h treatment time. Furthermore, this allowed us to compare the cell lines' various sensitivity levels to SR-4835. To understand the full effects of SR-4835, we performed a differential gene expression analysis at the global level using data from all five cell lines. We also analyzed each cell line separately to identify specific responses (Fig. 1B, Supplementary Table 2). The global analysis identified a very large number of differentially expressed genes (DEGs) upon SR-4835 treatment, with a higher proportion of downregulated genes (up: 4,402, down: 6,672). Notably, the majority of DEGs in the cell line specific analysis were also shared with the global analysis. Furthermore, the number of DEGs after SR-4835 treatment was higher in both cisplatin-resistant OC cell lines compared to their sensitive counterparts (ratio total DEGs: Caov-3 cis/Caov-3: 1.44; A2780 cis/A2780: 6.98). Next, we generated a SR-4835 target gene signature using the top 200 upregulated and top 200 downregulated genes from the global analysis (Fig. 1C). A strong SR-4835-dependent change in signature activity was evident in A2780 cis, Caov-3 and Caov-3 cis, while the magnitude of the effect was lower in A2780 and SK-OV-3. Thus, inhibition of CDK12/13 by SR-4835 in a near-patient situation regarding drug dosage and duration has very potent effects on the transcriptome in OC cells.

Molecular mechanism of differential gene expression by SR-4835

Previously, CDK12 inhibition or depletion has been shown to cause premature transcription termination, particularly at alternative IPA sites [16,17]. To evaluate this molecular mechanism of CDK12 inhibition by SR-4835 in OC, we re-analyzed the transcriptomic data from our study at the exon level enabling the enumeration of genes with alternative exon usage, i.e. genes expressed through different variants (Fig. 2A, Supplementary Table 3). Supplementary Fig. 2A

and B elucidate the bioinformatical analysis pipeline. Using the global analysis strategy, we identified 4,452 genes with significant alternative exon usage following SR-4835 treatment.

Next, we analyzed whether genes with alternative exon usage are downregulated through the recognition of IPA sites after CDK12 inhibition by SR-4835. To this end, we compared the exon- and gene-level analyses (Fig. 2B). In Caov-3, Caov-3 cis, and SK-OV-3, genes with alternative exon usage from the global analysis were predominantly downregulated at the gene expression level. However, in A2780 and A2780 cis, the number of up- and downregulated genes was more balanced. Additionally, the fraction of down-regulated genes at the exon level compared to the gene level was consistent, ranging from 22.2% (SK-OV-3) to 29.1% (A2780), with a mean of 25.3% ± 2.6%.

Furthermore, we examined the relationship between alternative exon usage and gene characteristics. Genes with significant alternative exon usage upon SR-4835 treatment were more than three times longer (median gene length 57,388 bp) than unaffected genes (non-significant alternative exon usage, median gene length 19,038 bp, Fig. 2C, top panel). In addition, these genes had a higher proportion of IPA sites (Fig. 2C, bottom panel). Spearman rank correlation showed that significant alternative exon usage (converted to a significance rank using the -log10 false discovery rate (FDR)) depended on gene length ($r_s = 0.34$; $p < 2.2e\text{-}16$) and IPA sites ($r_s = 0.30$; $p < 2.2e\text{-}16$) (Fig. 2D, left and right panel, respectively). Thus, premature transcription termination by CDK12/13 inhibition is more likely to occur in larger genes inherently containing more IPAs.

Implications of CDK12/13 inhibition by SR-4835 on biological signaling pathways

To further characterize the impact of SR-4835 on CDK12/13 function, focusing on affected biological pathways, we performed Reactome pathway over-representation analysis (ORA) using transcriptome data at the gene level (Fig. 3A, Supplementary Table 4). A global analysis revealed significantly over-represented pathways upon SR-4835 treatment (n = 50), as well as cell line-specific pathways for A2780 cis (n = 175), Caov-3 (n = 53), and Caov-3 cis (n = 201). However, no significantly over-represented pathways were found for parental A2780 and SK-OV-3. The

top 20 Reactome ORA pathways for A2780 cis, Caov-3, and Caov-3 cis are shown in Supplementary Fig. 3. In the global analysis, the top three significantly enriched pathways with the highest number of DEGs were related to transcriptional regulation by TP53, DNA repair and RHO GTPase effectors (Fig. 3A). These pathways showed also high DEG enrichment at the cell line-specific analyses for A2780 cis, Caov-3, and Caov-3 cis and less for parental A2780 and SK-OV-3 (Fig. 3B). Taken together, these results demonstrate that SR-4835 affects gene expression in several pathways.

Effect of CDK12/13 inhibition by SR-4835 on key DDR and carcinogenesis genes

Previously, a triple negative breast cancer (TNBC) study showed that CDK12/13 inhibition by SR-4835 did not have any effects on the expression of common carcinogenesis genes, while DDR pathway genes were downregulated [18]. As we could also detect the pathway DNA repair in the ORA Reactome analysis, we re-analyzed key representatives of this pathway. To have a better representation of the most common and aggressive OC subtype, HGSOC, in our analyses, the representative *BRCA1*-mutant cell line COV362 was included in our analyses. Cell confluence analyses with COV362 after SR-4835 treatment indicated an IC50 of 115.4 nM (95% CI: 96.05-138.6). Quantification of mRNA expression of key DNA repair genes after SR-4835 treatment for 24h revealed significant downregulation of *ATM*, *ATR*, and *BRCA1* in all cell lines (except *BRCA1* in SK-OV-3), while this effect was absent after cisplatin and olaparib treatment (Fig. 4A). For *FANCD2*, *FANCI* and *BRCA2* a uniform effect of SR-4835 was limited to Caov-3 and Caov-3 cis. SR-4835-mediated effects on other analyzed DDR (*RAD51*, *TP53*) and carcinogenesis genes (*CD44*, VEGFA, *KRAS, selected from* [18]) were absent or limited to single cell lines only (Supplementary Fig. 4A).

At the protein level, BRCA1 protein expression significantly decreased in most cell lines after SR-4835 treatment for 48h, and reduced ATM and ATR protein expression was observed in SK-OV-3, A2780 cis and COV362, as shown in Fig. 4B (for densitometrical analyses see Supplementary Fig. 4B). Thus, SR-4835-mediated mRNA downregulation of various DDR genes translates mostly to the protein level. Albeit SK-OV-3 have according to the DepMap portal the highest

CDK12 mRNA expression among all OC cell lines [25,26], a substantially increased protein expression was not detectable compared to remaining cell lines. From this data we concluded that SR-4835 is able to induce *BRCAness* in OC cells.

Synergism analysis of the combination treatments SR-4835/cisplatin and SR-4835/olaparib

Since treatment with SR-4835 lead to a decrease of DDR pathway gene expression (although not exclusively), we hypothesized that this effect may be beneficial to improve the action of the DNA damage-inducing agent cisplatin or the DDR (PARP) inhibitor olaparib. Sensitivity to cisplatin and olaparib respectively was assessed by determination of IC50 values for all cell lines (Supplementary Fig. 5). Interestingly, A2780 cis exhibited significantly lower sensitivity to olaparib than the parental cell line, A2780 ($p = 0.0013$). A similar tendency was observed for Caov-cis, though it was not statistically significant ($p = 0.0675$).

To elucidate a possible benefit of a combination therapy with SR-4835, we conducted cell viability and cell death assays on all six OC cell line models after mono- and co-treatments with SR-4835 and cell line-appropriate concentrations of cisplatin or olaparib (Fig. 5A). As expected from IC50 determinations, SR-4835 monotherapy had the highest effects on A2780 cis, Caov-3 and Caov-3 cis, moderate effects on A2780 and COV362, while SK-OV-3 were unresponsive to 90 nM SR-4835. SR-4835/cisplatin combination therapy compared to the cisplatin monotherapy showed significant increased responsiveness of parental and cisplatin-resistant A2780 and Caov-3 pairs in both cell viability and death assays. SR-4835/olaparib combination therapy vs olaparib monotherapy resulted in similar results for cell viability and less consistent results for cell death assays. To test whether the observed results of combination therapies are of additive or synergistic nature, Bliss synergy scores [27] were calculated. Only marginal and non-significant deviations from zero led us to conclude that the combination therapies SR-4835/cisplatin and SR-4835/olaparib act in an additive manner.

To support these findings at broader drug concentration ranges we performed dose-response cell confluence measurements after co-treatment of all six cell lines with either SR-4835/cisplatin (Fig. 5B) or SR-4835/olaparib (Fig. 5C) followed by assessment of drug synergism by the HSA

method. For the SR-4835/cisplatin combination (Fig. 5B), average HSA scores ranged from -5.8751 (COV362) to 4.5657 (Caov-3 cis) indicating that drug combinations act in an additive, and in the case of COV362, in a slightly antagonistic manner (Supplementary Table 5). For SR-4835/olaparib co-treatment (Fig. 5C), average HSA scores indicated minor antagonistic effects for SK-OV-3, COV362, A2780 and Caov-3 cis and additive effects for A2780 cis and Caov-3. From these experiments, we concluded that, despite induction of *BRCAness* through SR-4835, SR-4835/cisplatin and SR-4835/olaparib combination therapies do not act synergistically in OC cells.

DISCUSSION

Novel therapeutic options for OC patients who have progressed on platinum-based therapy are urgently needed. An interesting drug target candidate is CDK12, which is ubiquitously expressed in primary OC with slightly increased staining in metastatic lesions [22]. The CDK12/13 inhibitor SR-4835 works as a molecular glue leading to the disruption of the CDK12/CCNK complex by ubiquitin/proteasome-mediated degradation of CCNK [23]. We found that alternative exon usage after inactivation of CDK12 by SR-4835 correlates with gene length and the number of IPA sites. Indeed, genes within the HR pathway (e.g. BRCA1/2, ATM, ATR) are among the largest genes of the human genome, which provides sufficient explanation why the pathway DNA repair was found among the top regulated in the global transcriptome analysis.

Quereda et al. demonstrated strong synergistic effects of SR-4835 in combination with DNA-damaging chemotherapy and PARP inhibitors in triple-negative breast cancer [18]. This prompted us to comprehensively investigate the growth inhibitory effects and underlying molecular mechanisms of SR-4835 in several histologically distinct OC cell lines. It is intriguing to note that the cisplatin-resistant OC cell lines A2780 cis and Caov-3 cis had a tendency for an augmented response to SR-4835 in comparison to their parental, cisplatin-sensitive counterparts. Albeit there is a need to confirm this increased sensitivity to SR-4835 in additional cisplatin-resistant models, CDK12 might represent a vulnerability in late-stage OC. Mechanistically this could be explained by an increased transcription factor addiction in cisplatin-resistant OC [28]. Increased occupancy of transcription factors, such as PAX8 [29], at (de novo)

binding sites in late stage disease may result in a higher dependency to CDK12 for efficient transcription through its ability to phosphorylate the CTD of RNA polymerase II enabling a robust transcription elongation and transcript splicing. Thus, inhibition of CDK12 may open a new treatment strategy for platinum-resistant OC.

In general, combination therapies aim to decrease number and grade of adverse events through synergistic action of the drug at lower concentrations than those used for single agents. In OC, drug partners which increase genomic instability are sought by building on already OC-approved drug partners, such as platinum-based chemotherapy or PARP inhibitors. The mechanistic rationale for a SR-4835/cisplatin combination approach lies within the observed downregulation of the DDR pathway through the action of SR-4835 presumably leading to a higher amount of unrepaired, cisplatin-generated intra- and inter-strand crosslinks. However, when assessing the cisplatin/SR-4835 treatment in OC cells, we were unable to detect significant synergistic effects in three different assays (cell viability, death, and confluence). These additive effects contrast with the study of Quereda et al., who found strong synergism when testing the response of three TNBC cell lines to SR-4835/cisplatin treatment [18]. A possible reason for this discrepancy could be insufficient induction of genetic instability in our OC models despite potent inactivation of DDR pathways. However, also pre-incubation for 72h with low doses of SR-4835 followed by a combination treatment for 72h did not sensitize A2780 cis to cisplatin (Supplementary Fig. 7). Thus, further research to elucidate the molecular reasons for the lack of synergistic activity of SR-4835 when combined to cisplatin are needed. .

Similar additive, and in part antagonistic, effects were observed in the SR-4835/olaparib approach. Again, this is in contrast to the TNBC study, where high synergism for this combination was documented [18] and to a more recent study with ovarian patient-derived organoids with selected concentrations of another CDK12 inhibitor, THZ531, and olaparib [30]. Here, the rationale for using this combination approach is the generation of a *BRCAness* phenotype through the SR-4835-mediated downregulation of HR genes. This would substantially increase the number of patients benefiting from PARP inhibition therapy, in particular those with *BRCA1/2* wild type or with a low HRD score. Indeed, we found BRCA1 to be downregulated at both mRNA and protein levels in most cell lines, suggesting that *BRCA*ness is sufficiently induced by SR-

4835. However, one limitation of our study in this context is the rather short time of olaparib exposure (72h), which is an inherent limitation of most cell culture-based assays. PARP inhibition leads to constant accumulation of genomic aberrations over time, which finally results in cell death when a certain threshold is exceeded. Indeed, in the clinical setting the median time to onset of response for olaparib was reported to be 56.5 days in OC patients [31]. Thus, results from our short-term cell culture experiments are not necessary conclusive for possible synergistic effects in the clinical setting with long-term treatment regimens.

The present study demonstrates that dual CDK12/13 inhibition by SR-4835 exerts significant anticancer activity in OC cells, albeit substantial differences in IC50 values between the different cell lines were noted. The measured IC50 values for A2780, A2780 cis, Caov-3 and Caov-3 cis (37.73-64.77 nM) are higher than those observed in four TNBC cell lines (15.5 – 24.9 nM), which could however also be attributed to the different assays used [18]. In general, the genetic context of the analyzed OC cell lines could be explanatory for the different levels of sensitivity to SR-4835. *Dieter et al*. recently reported that colorectal tumors with *TP53* loss or inactivating mutations have a significantly higher sensitivity to NCT02, a cyclin K and CDK12 degrader, in a colorectal tumor spheroid model, whereas tumors with wild-type *TP53* were homogeneously resistant [32]. In our study, pathogenic mutations in *TP53* were detected in Caov-3 and Caov-3 cis (c.406C>T; p.Gln136Ter) and COV362 (c.659A>G; p.Tyr220Cys), and a likely pathogenic *TP53* mutation in SK-OV-3 (c.267delC; p.Ser90ProfsTer33), but no *TP53* mutations in A2780/A2780 cis. Thus, we cannot conclude on a correlation between SR-4835 sensitivity and *TP53* mutational status.

CONCLUSIONS

Here, we present a comprehensive pre-clinical study of the anticancer effects of the CDK12/13 inhibitor SR-4835 in OC cell lines. We find that inhibition of CDK12/13 has potent effects on the transcriptome and a possible increased reactivity of cisplatin-resistant compared to parental cells is intriguing. Albeit SR-4835 was able to downregulate key DDR genes including BRCA1, combination approaches of SR-4835 with cisplatin or olaparib had additive effects only.

MATERIAL AND METHODS

Cell lines and chemicals

A2780 (RRID:CVCL_0134) and A2780 cis (RRID:CVCL_1942) were purchased from Sigma-Aldrich (Vienna, Austria). Caov-3 (RRID:CVCL_0201) and its cisplatin-resistant derivative cell-line were kindly provided by Olli Carpén (University of Turku, Turku, Finland). COV362 cells (RRID:CVCL_2420) were kindly provided by Robert Zeillinger (Medical University of Vienna, Vienna, Austria). SK-OV-3 cells (RRID:CVCL_0532) were purchased from ATCC (LGC Standards GmbH, Wesel, Germany). To authenticate these cell lines, amplification of 15 STR loci and the sex-specific locus of amelogenin was performed at the Institute of Legal Medicine, Medical University of Innsbruck, as described previously [33]. The mutational characteristics of the cell lines are listed in Supplementary Table 1. Cells were routinely tested for mycoplasma contaminations using the qPCR-based Venor GeM qEP kit from Minerva Biolabs (Bio Products, Vienna, Austria). All cells were grown in the appropriate medium (RPMI or Dulbecco's modified Eagle's medium; PAA Laboratories; GE Healthcare, Munich, Germany) supplemented with 10 % fetal bovine serum (Biochrom, Cambridge, UK), 2 mM l-glutamine, and 1x penicillin/ streptomycin (Gibco; Life Technologies, Thermo Fisher Scientific, Waltham, MA).

SR-4835 and olaparib were purchased from THP Medical Products (Vienna, Austria; MedChem Express (MCE) HY-130250 and HY-10162, respectively) and dissolved in DMSO (Acros Organics BV. Janssen Pharmaceuticalaan, Geel, Belgium). Cisplatin (dissolved in 0.9% NaCl) was purchased from Sandoz Biopharmaceuticals and Oncology Injectables (Unterach, Austria).

RNA sequencing (transcriptome) analysis

Transcriptome analysis was performed 24h post-treatment with SR-4835 against vehicle (DMSO). Treatment concentration was 90 nM SR-4835 corresponding to the approximate double median IC50 concentrations of the five cell lines, thus allowing a better comparison of the effects on gene expression. Total cellular RNA was extracted as described previously [34]. Quality control, poly (A) enrichment, strand-specific library preparation, and sequencing (paired-end 150 bp, >20 million read pairs per sample) were performed by Novogene (Cambridge, UK). Adapter

filtering and quality trimming of the reads was performed using BBMap/BBDuk (version 38.96). Data analysis was performed in R (version 4.1.3). Read alignment (GENCODE release 39, GRCh38.p13) and counting were performed using the R subread package (version 2.8.2). Differential gene expression and exon usage analyses were performed using the limma package (version 3.50.1). For the differential exon usage analysis, we filtered the exon annotation (GENCODE release 39) to avoid multiple testing of the same region. Specifically, all exons were chopped into non-overlapping regions followed by filtering of regions with low expression levels (< 0.1 RPKM or less than 5 % of the median gene expression) and re-fusing of directly adjacent regions with similar gene expression levels. Thus, the term exon used in this analysis does not necessarily refer to a complete individual exon of a transcript. Pathway overrepresentation analysis was performed using the ReactomePA package (version 1.38.0), and gene set activity scores (ssGSEA method) were calculated using GSVA (1.44.4). Gene length was determined by calculating the distance from the first to the last expressed exon. Annotation of the polyadenylation (poly (A)) sites was obtained from the GENCODE release.

Cell confluence measurements for IC50 and synergism determinations

For IC50 determination of SR-4835, olaparib and cisplatin cells were seeded in a 96-well plate (Corning, Corning, NY) and treated with various concentrations of SR-4835, olaparib and cisplatin or vehicle for 72 hours (SK-OV-3: 1-2 E3 cells/well, 0-3000 nM SR-4835 (dilution factor (df) 2.5), 0-400 µM cisplatin (df 4), olaparib 0-625 µM (df 2.5); COV362: 2-3 E3 cells/well, 0-3000 nM SR-4835 (df 2.5), 0-400 µM cisplatin (df 4), olaparib 0-1200 µM (df 4); A2780 and A2780 cis: 6 E3 cells/well each, 0-1200 nM SR-4835 (df 2-2.5), 0-400 µM cisplatin (df 4), olaparib 0-300 µM (df 4); Caov-3 and Caov-3 cis: 1 E4 cells/well each, 0-5000 nM SR-4835 (df 2-4), 0-400 µM cisplatin (df 4), olaparib 0-600 µM (df 4). The Incucyte Live-Cell Analysis System (Essen BioScience, Ann Arbor, MI, USA) was used to measure confluence, expressed as area fraction, using the artificial intelligence (AI) confluence algorithm. The measured area was averaged over four image fields per well for each cell line. Raw data (% average confluence) at time point 72h post-treatment was normalized in GraphPad Prism v10 by setting the lowest value to 0% and the highest value to 100% for each experiment separately. IC50 Best-fit values were then calculated

by using the log(inhibitor) vs. normalized response function of GraphPad Prism and converted to pIC50, i.e. –log[M] values. The pIC50 value indicates the degree of sensitivity a cell line exhibits toward a drug. Highest Single Agent (HSA) synergy analyses between SR-4835/cisplatin and SR-4835/olaparib were calculated by Combenefit software (v2.021) [35]. As this software requires equal drug concentrations, missing values (as a result of using different drug concentration ranges and dilutions factors) were imputed by using the synergyfinder (v3.14.0) package in R (v4.4.3) with the ReshapeData function and the impute method argument set to Random Forest (rf). HSA scores were computed for all drug combinations, and the significance of their mean deviation from zero was evaluated by one-sided Student's t-tests. HSA scores ranging between -5 and +5 are usually considered to indicate additive drug action [36].

Determination of cell viability and death and synergism determinations

For cell viability and death assays, cells were treated with 90 nM SR-4835, cisplatin (0.3 µM: Caov-3; 1.0 µM: A2780; 3.0 µM: A2780 cis, Caov-3 cis, COV362, SK-OV-3) and olaparib (10 µM: A2780, A2780 cis, Caov-3, Caov-3 cis; 30 µM: COV362, SK-OV-3) for 96 hours. Cell viability was assessed using the 3-(4,5-dimethyl-2-thiazolyl)-2,5-diphenyl-2H-tetrazolium bromide (MTT) assay (Sigma-Aldrich, Vienna, Austria) as previously described [34]. Cell death was measured by staining the cells with propidium iodide/Triton X-100 (Sigma-Aldrich) and flow cytometry using a Beckman Coulter Cytomics FC-500 as previously described [37]. Synergism was quantified using Bliss scores [27], and deviations from zero were evaluated based on propagated uncertainties.

DNA sequencing analysis

For the genetic characterization of the cell lines used in this study, DNA sequencing was performed by IMGM Laboratories GmbH (Martinsried, Germany). Sequencing libraries were generated using the QIAseq Targeted DNA Panel (Human Comprehensive Cancer Panel). This panel provides ultrasensitive variant detection by integrating unique molecular indices (UMIs) into a single gene-specific, primer-based targeted enrichment method. DNA sequencing was performed on an Illumina NovaSeq 6000 next-generation sequencing system (2x 150 bp PE run).

Data analysis was performed using SeqNext software (Sequence Pilot 5.2.0 Build 507; JSI Medical Systems, Ettenheim, Germany).

Quantitative real-time PCR analysis of mRNA expression

Total cellular RNA extraction, reverse transcription and quantitative real-time PCR (qPCR) using the Quant Studio 6 Flex real-time PCR system with QuantStudio real-time PCR software were performed as previously described [34]. Primers and probes for ATM (Hs00175892_m1), ATR (Hs00354807_m1), B2M (reference gene; Hs00187842_m1), BRCA1 (Hs01556193_m1), FANCD2 (Hs00276992_m1), FANCI (Hs01105308_m1), KRAS (Hs00364282_m1), OAZ1 (reference gene; Hs00427923_m1), RAD51 (Hs00153418_m1), TP53 (Hs01034249_m1), VEGFA (Hs00900055_m1) were purchased from Applied Biosystems (Foster City, CA, USA). B2M was used as a housekeeping gene for A2780, A2780 cis, COV362 and SK-OV-3. OAZ1 served the same purpose for Caov-3 and Caov-3 cis. The OVCAR3 cell line was used as a positive control and SKOV6 was used for the standard curve.

Western blot analysis

Cell lysates were prepared by direct lysis in 1.5x NuPAGE LDS sample buffer (Fisher Scientific, Vienna, Austria), followed by sonication to reduce viscosity. A total of 20 µg protein per sample was loaded onto 3 to 8% Tris-Acetate NuPAGE protein gels (Thermo Fisher Scientific) for electrophoretic separation under reducing conditions. Proteins were transferred overnight at constant 12 V on 0.4 µm Amersham Protran nitrocellulose membranes (GE Healthcare, Vienna, Austria) and blocked for 3 h with StartingBlock blocking buffer (TBS; Fisher Scientific). Primary antibody incubation was performed overnight at 4°C in blocking buffer containing 0.2 % (v/v) Tween 20 (Serva, Heidelberg, Germany) and the following antibodies: mouse anti-BRCA1 (D-9, 1:100), mouse anti-ATM (G-12, 1:200), mouse anti-ATR (C-1, 1:200), mouse anti-vinculin (H-10, 1:5000) (all from Santa Cruz Biotechnology, Szabo-Scandic, Vienna, Austria) and rabbit anti-CDK12 (Cell Signaling, Leiden, The Netherlands). Detection was performed with goat IgG anti-mouse or anti-rabbit IgG (H+L)-HRPO (1:10,000, Jackson ImmunoResearch, Dianova, Hamburg, Germany) and SuperSignal West Femto Maximum Sensitivity ECL substrate (Pierce,

Fisher Scientific) on a ChemiDoc MP imaging system (Bio-Rad, Vienna, Austria). Densitometrical analysis was performed using Bio-Rad Image Lab software on images taken with the “auto exposure intense bands” function. Uncropped and unmodified Western blot images corresponding to Fig. 4B can be found in Supplementary Fig. 6.

Statistics

The following statistical tests were used in this study and are specified in the legend of each figure: Mann-Whitney U test, Spearman´s rank correlation, one- and two-way ANOVA with uncorrected Fisher´s LSD test for multiple comparison. Statistical analyses were done using IBM SPSS Statistics for Windows version 26.0 and GraphPad Prism version 10.1.2. P-values ≤ 0.05 were considered statistically significant and encoded as follows: * $p \leq 0.05$; ** $p \leq 0.01$; *** $p \leq 0.001$; **** $p \leq 0.0001$. Values are presented as mean ± standard deviation (SD), standard error of the mean (SEM) or with 95% confidence intervals (CI).

REFERENCES

1. Sung, H. *et al.* Global Cancer Statistics 2020: GLOBOCAN Estimates of Incidence and Mortality Worldwide for 36 Cancers in 185 Countries. *CA Cancer J Clin* **71**, 209–249 (2021).
2. Karam, A. *et al.* Fifth Ovarian Cancer Consensus Conference of the Gynecologic Cancer InterGroup: first-line interventions. *Ann Oncol* **28**, 711–717 (2017).
3. Vergote, I. *et al.* Treatment algorithm in patients with ovarian cancer. *Facts Views Vis Obgyn* **12**, 227–239 (2020).
4. Moore, K. *et al.* Maintenance Olaparib in Patients with Newly Diagnosed Advanced Ovarian Cancer. *N Engl J Med* **379**, 2495–2505 (2018).
5. González-Martín, A. *et al.* Niraparib in Patients with Newly Diagnosed Advanced Ovarian Cancer. *N Engl J Med* **381**, 2391–2402 (2019).
6. Friedlander, M. *et al.* Clinical trials in recurrent ovarian cancer. *Int J Gynecol Cancer* **21**, 771–775 (2011).

7. Miller, R. E., El-Shakankery, K. H. & Lee, J.-Y. PARP inhibitors in ovarian cancer: overcoming resistance with combination strategies. *J Gynecol Oncol* **33**, e44 (2022).
8. Greenleaf, A. L. Human CDK12 and CDK13, multi-tasking CTD kinases for the new millenium. *Transcription* **10**, 91–110 (2019).
9. Sokol, E. S. *et al.* Pan-Cancer Analysis of CDK12 Loss-of-Function Alterations and Their Association with the Focal Tandem-Duplicator Phenotype. *Oncologist* **24**, 1526–1533 (2019).
10. Popova, T. *et al.* Ovarian Cancers Harboring Inactivating Mutations in CDK12 Display a Distinct Genomic Instability Pattern Characterized by Large Tandem Duplications. *Cancer Res* **76**, 1882–1891 (2016).
11. Bajrami, I. *et al.* Genome-wide profiling of genetic synthetic lethality identifies CDK12 as a novel determinant of PARP1/2 inhibitor sensitivity. *Cancer Res* **74**, 287–297 (2014).
12. Blazek, D. The cyclin K/Cdk12 complex: an emerging new player in the maintenance of genome stability. *Cell Cycle* **11**, 1049–1050 (2012).
13. Blazek, D. *et al.* The Cyclin K/Cdk12 complex maintains genomic stability via regulation of expression of DNA damage response genes. *Genes Dev* **25**, 2158–2172 (2011).
14. Joshi, P. M., Sutor, S. L., Huntoon, C. J. & Karnitz, L. M. Ovarian cancer-associated mutations disable catalytic activity of CDK12, a kinase that promotes homologous recombination repair and resistance to cisplatin and poly(ADP-ribose) polymerase inhibitors. *J Biol Chem* **289**, 9247–9253 (2014).
15. Ekumi, K. M. *et al.* Ovarian carcinoma CDK12 mutations misregulate expression of DNA repair genes via deficient formation and function of the Cdk12/CycK complex. *Nucleic Acids Res* **43**, 2575–2589 (2015).
16. Krajewska, M. *et al.* CDK12 loss in cancer cells affects DNA damage response genes through premature cleavage and polyadenylation. *Nat Commun* **10**, 1757 (2019).
17. Dubbury, S. J., Boutz, P. L. & Sharp, P. A. CDK12 regulates DNA repair genes by suppressing intronic polyadenylation. *Nature* **564**, 141–145 (2018).
18. Quereda, V. *et al.* Therapeutic Targeting of CDK12/CDK13 in Triple-Negative Breast Cancer. *Cancer Cell* **36**, 545-558.e7 (2019).

19. Johnson, S. F. *et al.* CDK12 Inhibition Reverses De Novo and Acquired PARP Inhibitor Resistance in BRCA Wild-Type and Mutated Models of Triple-Negative Breast Cancer. *Cell Rep* **17**, 2367–2381 (2016).
20. Wang, C. *et al.* CDK12 inhibition mediates DNA damage and is synergistic with sorafenib treatment in hepatocellular carcinoma. *Gut* **69**, 727–736 (2020).
21. Iniguez, A. B. *et al.* EWS/FLI Confers Tumor Cell Synthetic Lethality to CDK12 Inhibition in Ewing Sarcoma. *Cancer Cell* **33**, 202-216.e6 (2018).
22. Cheng, L. *et al.* Dual Inhibition of CDK12/CDK13 Targets Both Tumor and Immune Cells in Ovarian Cancer. *Cancer Res* **82**, 3588–3602 (2022).
23. Houles, T. *et al.* The CDK12 inhibitor SR-4835 functions as a molecular glue that promotes cyclin K degradation in melanoma. *Cell Death Discov* **9**, 459 (2023).
24. Rajan, N. *et al.* Differential activity of specific inhibitors of transcription regulating cyclin-dependent kinases in thyroid cancer cells. *Endocr Relat Cancer* ERC-24-0124 (2025) doi:10.1530/ERC-24-0124.
25. CDK12 DepMap Gene Summary. https://depmap.org/portal/gene/CDK12?tab=characterization&characterization=expression.
26. Arafeh, R., Shibue, T., Dempster, J. M., Hahn, W. C. & Vazquez, F. The present and future of the Cancer Dependency Map. *Nat Rev Cancer* **25**, 59–73 (2025).
27. Bliss, C. I. The Toxicity of Poisons Applied Jointly. *Annals of Applied Biology* **26**, 585–615 (1939).
28. Davies, M., Boyce, M. & Conway, E. Short circuit: Transcription factor addiction as a growing vulnerability in cancer. *Curr Opin Struct Biol* **89**, 102948 (2024).
29. Santos-Pereira, J. M., Carnero, A. & Muñoz-Galván, S. Integrative multi-omic analysis reveals a PAX8-driven gene network linking tumor stemness to therapy response in ovarian cancer. *NAR Genom Bioinform* **7**, lqaf113 (2025).
30. Cesari, E. *et al.* Dual inhibition of CDK12 and CDK13 uncovers actionable vulnerabilities in patient-derived ovarian cancer organoids. *J Exp Clin Cancer Res* **42**, 126 (2023).
31. Kaufman, B. *et al.* Olaparib monotherapy in patients with advanced cancer and a germline BRCA1/2 mutation. *J Clin Oncol* **33**, 244–250 (2015).

32. Dieter, S. M. *et al.* Degradation of CCNK/CDK12 is a druggable vulnerability of colorectal cancer. *Cell Rep* **36**, 109394 (2021).
33. Parson, W. *et al.* Cancer cell line identification by short tandem repeat profiling: power and limitations. *FASEB J* **19**, 434–436 (2005).
34. Fiegl, H. *et al.* Dubious effects of methadone as an 'anticancer' drug on ovarian cancer cell-lines and patient-derived tumor-spheroids. *Gynecol Oncol* **165**, 129–136 (2022).
35. Di Veroli, G. Y. *et al.* Combenefit: an interactive platform for the analysis and visualization of drug combinations. *Bioinformatics* **32**, 2866–2868 (2016).
36. Malyutina, A. *et al.* Drug combination sensitivity scoring facilitates the discovery of synergistic and efficacious drug combinations in cancer. *PLoS Comput Biol* **15**, e1006752 (2019).
37. Nicoletti, I., Migliorati, G., Pagliacci, M. C., Grignani, F. & Riccardi, C. A rapid and simple method for measuring thymocyte apoptosis by propidium iodide staining and flow cytometry. *J Immunol Methods* **139**, 271–279 (1991).

FUNDING

This work was supported by the Verein zur Krebsforschung in der Frauenheilkunde.

ACKNOWLEDGMENTS

We thank Kathrin Ausserlechner, Brigitte Greiderer-Kleinlercher, Petra Hechenberger, Stefanie Rainer, Sarah Ritscher and the team of the High Throughput DNA Database Laboratory, Institute of Legal Medicine, Medical University of Innsbruck for their excellent technical assistance and Kaisa Huhtinen, Olli Carpén and Robert Zeillinger for providing cell lines.

AUTHOR CONTRIBUTIONS

H.F. and C.M. developed the concept and designed the study. L.H., F.H., F.S., I.T., V.W., M.J.A., W.P, S.S., A.G.Z., C.M., and H.F. were involved in the data acquisition and quality control of the data and algorithms. L.H., F.H., F.S., I.T., V.W., M.J.A., W.P, A.G.Z., C.M., and H.F. analyzed and interpreted the data. L.H., F.H., F.S and H.F. performed statistical analyses and prepared

the manuscript. L.H., F.H., F.S., I.T., V.W., M.J.A., W.P, S.S., A.G.Z., C.M., and H.F. edited the manuscript and reviewed the final version.

DATA AVAILABILITY STATEMENT

The data supporting the findings of this study are provided in the Supplementary Information of this article or are available from the corresponding author upon request. The datasets generated and/or analysed during the current study are available in the ArrayExpress repository under accession number E-MTAB-15987 (https://www.ebi.ac.uk/biostudies/ArrayExpress/studies/E-MTAB-15987). Raw sequencing reads (FASTQ) can be retrieved from the European Nucleotide Archive under accession number PRJEB93935 (https://www.ebi.ac.uk/ena/browser/view/PRJEB93935).

CONFLICT OF INTEREST

The authors declare that they have no known competing financial interests or personal relationships that could have appeared to influence the work reported in this paper. However, the following authors receive financial support for the specified activities: VW reports honoraria from Roche, Novartis; travel expenses from Roche; participation on advisory boards from Novartis. CM reports consulting fees from Roche, Novartis, Amgen, MSD, PharmaMar, AstraZeneca, GSK, Seagen; honoraria from Roche, Novartis, Amgen, MSD, PharmaMar, AstraZeneca, GSK, Seagen; travel expenses from Roche, AstraZeneca; participation on advisory boards from Roche, Novartis, Amgen, MSD, AstraZeneca, Pfizer, PharmaMar, GSK, Seagen. AGZ reports consulting fees from Amgen, AstraZeneca, GSK, MSD, Novartis, PharmaMar, Roche-Diagnostics, Seagen; honoraria from Amgen, AstraZeneca, GSK, MSD, Novartis, PharmaMar, Roche, Seagen; travel expenses from AstraZeneca, Gilead, Roche; participation on advisory boards from Amgen, AstraZeneca, GSK, MSD, Novartis, Pfizer, PharmaMar, Roche, Seagen. The other authors have no conflict of interest.

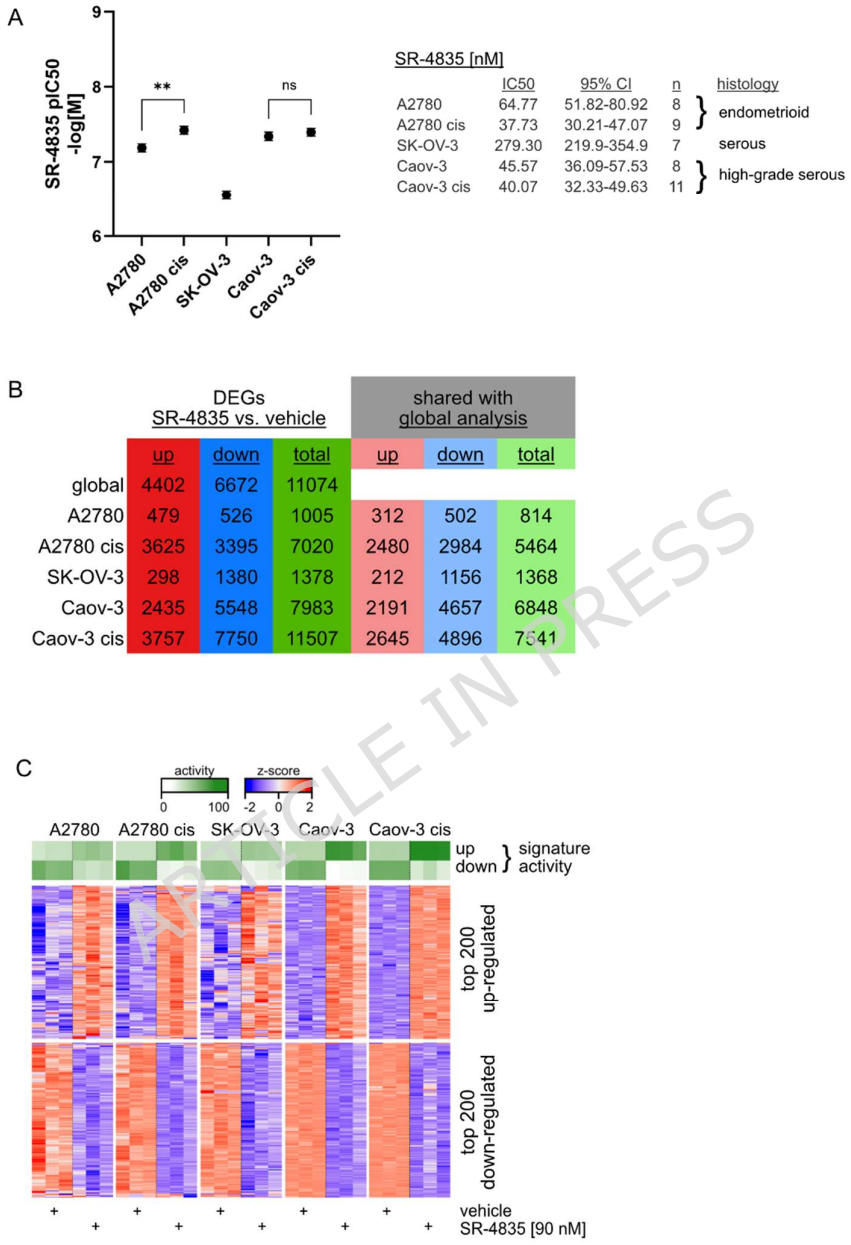

Figure 1: Proliferative and gene expression effects of CDK12/13 inhibition by SR-4835 in OC cell lines: (A) IC50 determination in A2780, A2780 cis, SK-OV-3, Caov-3, Caov-3 cis OC cell lines by confluence measurements after treatment with SR-4835 for 72 hours. Graph depicts the pIC50 mean value ±SEM in -log[M], table gives the converted IC50 values in [nM] with their respective 95% confidence intervals. ** p<0.01; ns, not significant by one-way ANOVA with

uncorrected Fisher´s LSD multiple comparison testing. Note, IC50 values in A2780 cis and Caov-3 cis were determined in the absence of cisplatin. **(B)** Differential gene expression analysis of SR-4835 vs. vehicle (DMSO)-treated cells. Cells were treated with 90 nM SR-4835 for 24h followed by RNA sequencing using a poly(A)-enriched cDNA library. Shown are the global analysis (where all five indicated cell lines were joined in the statistical model) and the cell line-specific analyses with up- and down-regulated genes, and total differential expressed genes (DEGs), as well as the respective number of shared differential expressed genes with the global analysis. **(C)** The top 200 up- and downregulated genes from the global analysis (B) were used as a gene set to analyze SR-4835´s activity in the respective OC cell lines. To this end gene set enrichment was performed for each sample and the resulting signature activity is shown on top of the heatmaps of the selected genes. Z-score scaling is performed separately for each cell line to highlight the effect of SR-4835.

A

Genes with alternative exon usage
SR-4835 vs. vehicle

	significant	Shared with global analysis
global	4452	
A2780	184	151
A2780 cis	4601	2778
SK-OV-3	562	468
Caov-3	1920	1762
Caov-3 cis	4213	3203

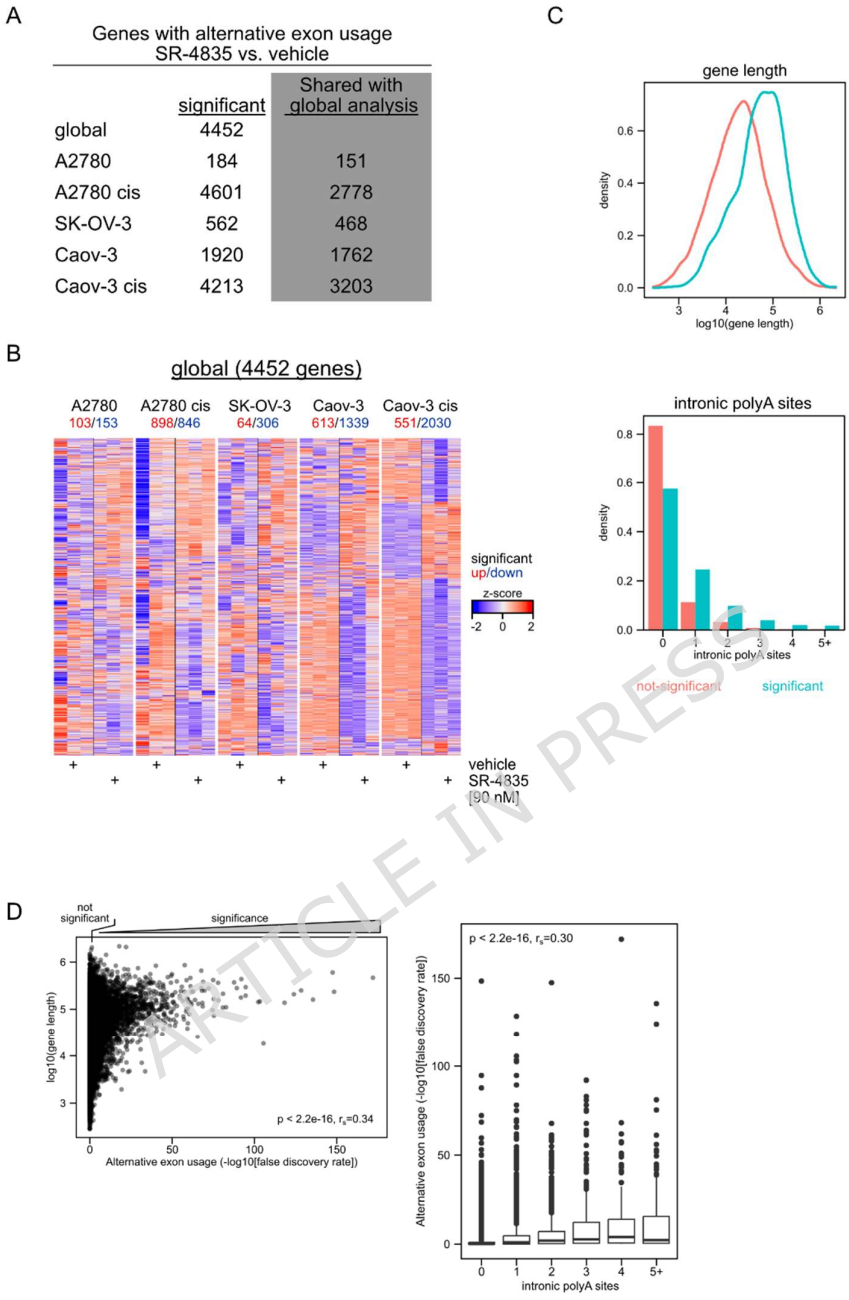

Figure 2: Differential gene expression on the exon level after treatment with SR-4835. (A) Re-analysis of the transcriptomic data on the exon level. Shown are the numbers of genes with significant alternative exon usage of SR-4835 treated cells vs. vehicle (DMSO) in the global analysis, specifically for each cell line and the shared number of genes with alternative exon usage with the global analysis. (B) Cell line specific heatmap of the 4452 genes with alternative

exon usage identified in the global analysis. Numbers on top are significantly up- or downregulated genes at the gene level. Z-score scaling is performed separately for each cell line to highlight the effect of SR-4835. (C) Density histogram plot (top panel) showing the log10 gene length and density bar plot (lower panel) showing the number of IPA sites/gene of genes with (significant) and without (not significant) alternative exon usage. (D) Correlation plots showing the log10 gene length (left) or the number of IPA sites/gene (right) vs the –log10 false discovery rate (FDR)-ranked genes with alternative exon usage. Statistical correlation analysis was done by Spearman r testing (r_s, goodness of fit; p, significance value).

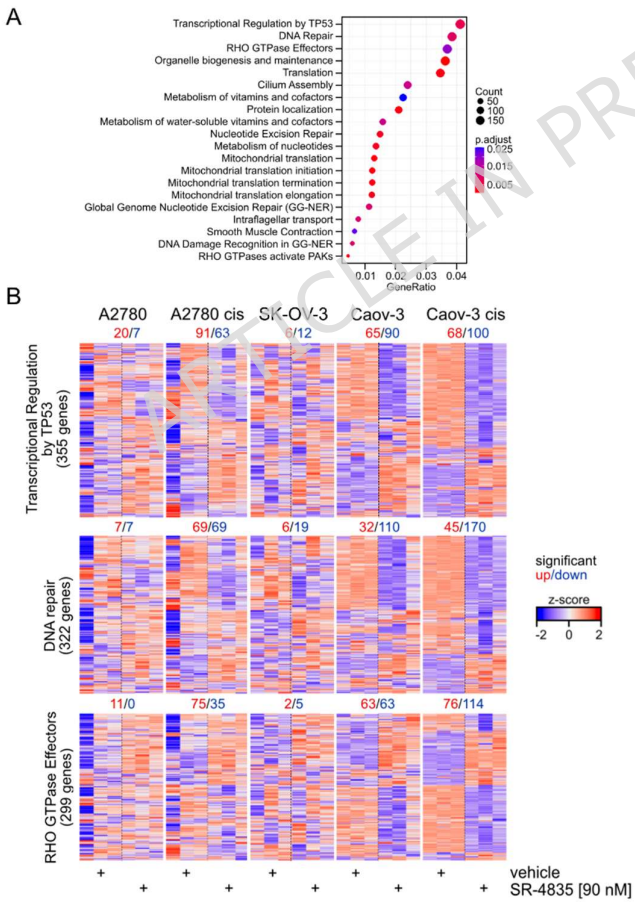

Figure 3: Pathway analysis of differentially expressed genes after SR-4835 treatment. (A) Pathway analysis of DEGs by Reactome ORA using the global analysis. The top 20 significant pathways ranked by the number of DEGs in this pathway (GeneRatio) are shown. (B) Cell line-specific heatmaps for the identified top 3 pathways in the global analysis. The number of up- and downregulated genes in the respective pathways are shown on top of each heatmap.

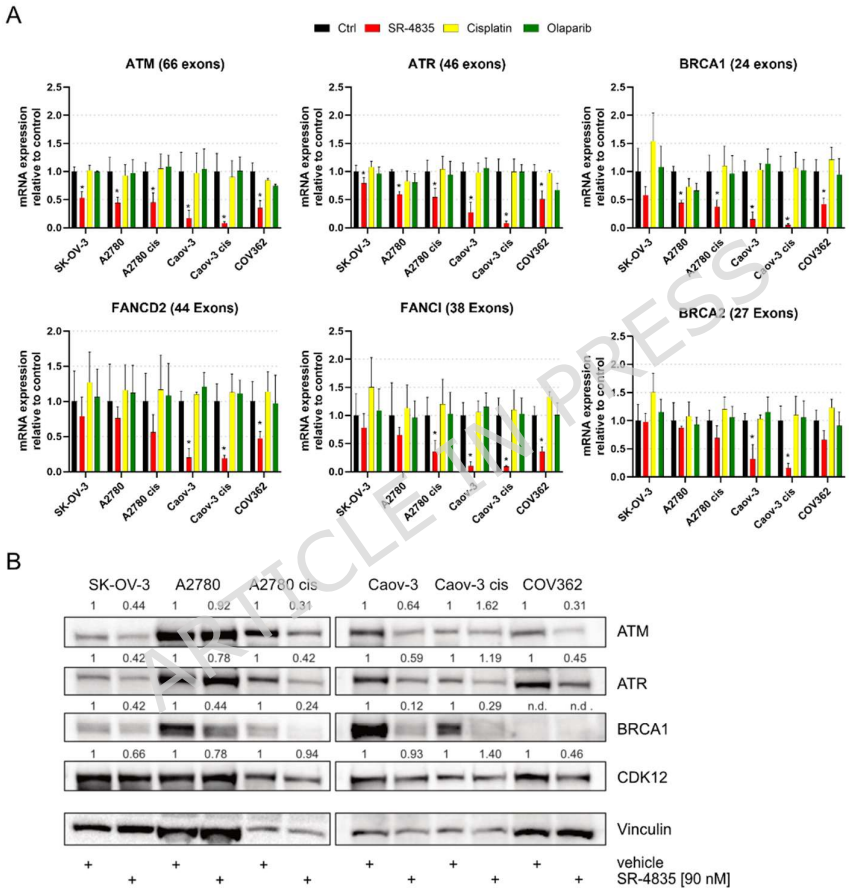

Figure 4: Expression of selected genes involved in DNA damage response (DDR) after SR-4835 treatment. (A) mRNA expression data for selected genes, as indicated, following treatment with 90 nM SR-4835 or 0.3 µM (Caov-3), 1 µM (A2780), 3 µM (SK-OV-3, COV362, A2780 cis, Caov-3 cis) cisplatin or 10 µM (A2780, A2780 cis, Caov-3, Caov-3 cis), 30 µM (SK-OV-3, COV362) olaparib. Bars indicate mean ±SD (n≥3). Statistical significance was calculated by

Mann-Whitney U test; *p<0.05. (B) Western blot analyses for ATM, ATR, BRCA1, and CDK12 after treatment with 90 nM SR-4835 for 48h. A representative immunoblot is shown (n=3). COV362 are negative for BRCA1 (*BRCA1* frameshift mutation). Mean values of the densitometrical band analyses (normalized to the loading control Vinculin) are shown on top for each sample and protein of interest.

A

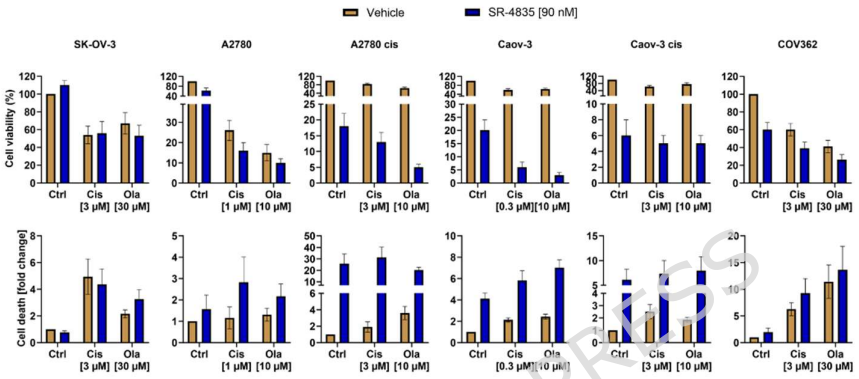

		SK-OV-3		A2780		A2780 cis		Caov-3		Caov-3 cis		COV362	
Mono-therapies	Vehicle vs. SR-4835	***	*	***	ns	*	**	***	*	***	*	***	*
	Vehicle vs. Cisplatin	***	*	***	ns	*	***	***	*	***	*	***	ns
	Vehicle vs. Olaparib	***	*	***	ns	*	*	***	ns	***	*	***	*
	SR-4835 vs. Cisplatin	***	*	***	ns	*	**	***	*	***	*	ns	ns
	SR-4835 vs. Olaparib	***		***	ns	*	ns	***	ns	***	*	**	*
Mono- vs. Combination therapy	Cisplatin vs. Cisplatin + SR-4835	ns	ns	***	*	*	**	***	*	***	*	***	ns
	Olaparib vs. Olaparib + SR-4835	ns	ns	**	*	*	ns	***	ns	***	*	***	ns
	SR-4835 vs. Cisplatin + SR-4835	***	*	***	*	ns	ns	**	*	ns	ns	***	*
	SR-4835 vs. Olaparib + SR-4835	***	*	***	ns	ns	ns	***	*	ns	ns	***	*

		SK-OV-3	A2780	A2780 cis	Caov-3	Caov-3 cis	COV362
SR-4835 & Cisplatin	Bliss Score	-0.034	-0.0012	-0.0212	-0.056	0.0128	0.03
	Significance	ns	ns	ns	ns	ns	ns
	Bliss Score	0.0431	0.0281	0.3071	0.0573	0.0718	0.0916
	Significance	ns	ns	ns	ns	ns	ns
SR-4835 & Olaparib	Bliss Score	-0.207	0.007	-0.0652	-0.096	0.0044	0.014
	Significance	ns	ns	ns	ns	ns	ns
	Bliss Score	0.0324	0.0215	0.1939	0.0692	0.0785	0.1341
	Significance	ns	ns	ns	ns	ns	ns

cell viability cell death

Bliss Score
>0 synergistic
~0 additive
<0 antagonistic

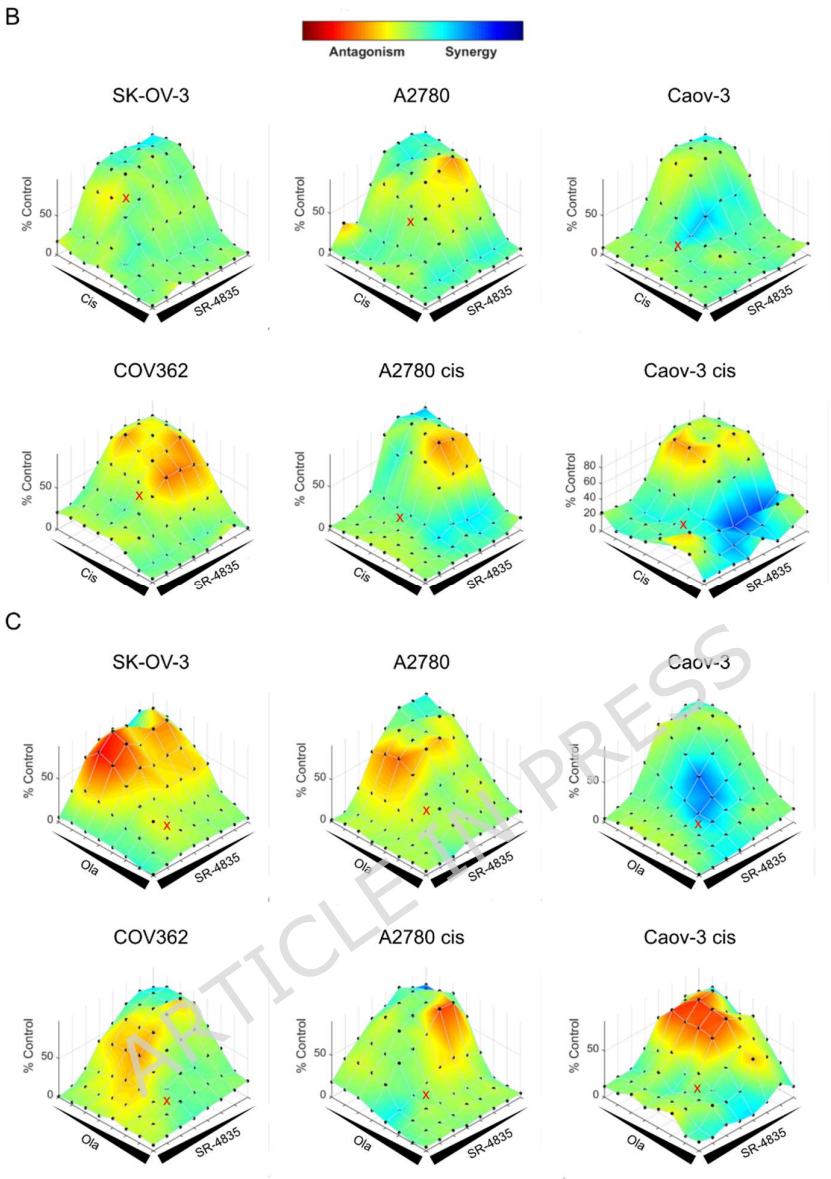

Figure 5: Effects of cisplatin or olaparib with SR-4835 combination therapies. (A) Cell viability (MTT assay, top bar plots) and cell death (PI/ flow cytometry, bottom bar plots) was assessed after OC cell line treatment with either 90 nM SR-4835 alone, cisplatin or olaparib (monotherapies) or in combination (concentrations as indicated). Top table indicates statistical significances of the various treatment comparisons assessed by Mann-Whitney U test. Bottom table indicates Bliss scores for synergism analysis. Statistical significance of the mean deviation from zero was evaluated by one-sided Student's t-tests. (B, C) HSA synergy analyses of drug

dose-response of SR-4835 with cisplatin (n=4) (B) or olaparib (n=3) (C) assessed by confluence measurements with the Incucyte live cell imaging system. Red crosses indicate the specific concentrations used in Fig. 5A. Missing values needed for HSA synergy analysis (due to the use of different concentrations ranges and dilution factors) were imputed using the random forest method. The following concentration ranges and dilution factors (df) are depicted: SR-4835: 0-1200 nM (df=2.5) for SK-OV-3, A2780, COV362, A2780 cis and 0-400 nM (df= 2) for Caov-3 and Caov-3 cis; cisplatin: 0-400 µM (df=4) for SK-OV-3, COV362, A2780 cis, Caov-3 cis and 0-100 µM (df=4) for A2780, Caov-3; olaparib: 0-300 µM (df=4) for all cell lines.